

# Thermal problems during start-up of cage induction motors

Jan MRÓZ and Piotr BOGUSZ\*

Rzeszów University of Technology, The Faculty of Electrical and Computer Engineering,  
al. Powstańców Warszawy 12, 35-959 Rzeszów, Poland

**Abstract.** This article considers the problem of the rise in temperature of the windings of an induction motor during start-up. Excessive growth of thermal stresses in the structure of a cage winding increases the probability of damage to the winding of the rotor. For the purpose of analysis of the problem, simplified mathematical relationships are given, enabling the comparison of quantities of energy released in a rotor winding during start-up by different methods. Also, laboratory tests were carried out on a specially adapted cage induction motor enabling measurement of the temperature of a rotor winding during its operation. Because there was no possibility of investigating motors in medium- and high-power drive systems, the authors decided to carry out tests on a low-power motor. The study concerned the start-up of a drive system with a 4 kW cage induction motor. Changes in the winding temperature were recorded for three cases: direct online start-up, soft starting, and the use of a variable-frequency drive (VFD). Conclusions were drawn based on the results obtained. In high-power motors, the observed phenomena occur with greater intensity, because of the use of deep bar and double cage rotors. For this reason, indication is made of the particular need for research into the energy aspects of different start-up methods for medium- and high-power cage induction motors in conditions of prolonged start-up.

**Key words:** cage induction motor; direct start-up; softstart; winding temperature.

## 1. Introduction

In medium and high-power drive systems, an important factor in the selection of a suitable electric motor is the required start-up properties. These may be determined by the design of the motor (deep bar rotor, double cage rotor), but also by the choice of start-up method (direct online, soft starting, VFD). High inertia of the drive system and a large load torque may lengthen the start-up time, which can lead to damage to the motor. The thermal effects of prolonged start-up are highly significant for the reliability of the drive, since irrespective of the choice of start-up method, unfavourable deformations occur in the heated elements of the cage winding, accompanied by damaging mechanical stresses. In these conditions the cage winding of the motor may be put at significant risk of damage, due to overheating of the winding and the appearance of thermally induced mechanical stress. Initial damage to the rotor cage winding usually takes the form of fissures and cracks. Such minor damage to the cage does not alter the motor's starting torque and is not easily noticed by operating personnel, as it does not affect the duration of start-up. Over time, however, it develops into fractures and melting of the bars of the cage winding. For this reason, an important area in which developments have recently been made is diagnostics of the rotor windings of large induction motors [1, 2], including those fed by inverters [3]. Since prolonged start-up of a cage motor is the source of the highest stresses, constructors and designers of cage induction motors seek various methods to counteract its adverse effects.

Work has been done on thermal and ventilation issues in electrical machines [4], and thermal analysis is becoming an increasingly important part of motor design algorithms [5–7]. Another direction of work aimed at improving the resistance of cage windings involves changes to the cage winding material and the shape of rotor slots [8–11]. Work is also ongoing on modernising the design of cage windings to increase their resistance to damage [12–15]. Some of the adverse effects of the starting of an induction motor can also be reduced by an appropriate choice of start-up method. The problems associated with prolonged start-up of cage motors when indirect start-up methods are used have been analysed in many studies, but the analysis was based almost exclusively on simulations. Reference [16] describes the distribution of energy released in particular elements of the windings of an induction motor. Simulation results are presented for a 320 kW deep bar cage motor, during both direct online start-up and soft starting. Reference [17] describes a simulation of the temperature field of the rotor of a 320 kW double cage motor during direct online start-up and soft starting. Reference [18] contains an analysis of the soft starting of a 5 hp cage induction motor. A model is presented for a drive system with a cage induction motor connected to a soft starter, enabling simulations of the transient electromechanical state during start-up. The simulation results were compared with the results of experiments performed for different soft starter control profiles. The problem of the heating of the windings was also signalled in this work, but only through the calculation of a stator heating index. This was determined as an integral of the square of the current in the stator during start-up. Meanwhile, as has already been noted, in medium- and high-power drive systems a prolonged start-up process can lead to unfavourable deformations of the heated elements of the cage winding, accompanied by mechanical stresses.

\*e-mail: pbogu@prz.edu.pl

Manuscript submitted 2020-12-23, revised 2021-02-07, initially accepted for publication 2021-02-16, published in June 2021

Experimental tests on high-power motors are subject to a number of logistical problems, since they usually have to take place in industrial conditions, which makes the experiments expensive to perform. For this reason, there are relatively few existing reports on experimental research relating to temperature rise in high-power cage induction motors [19–21].

In the present study, comparative experiments were performed with a cage induction motor subjected to soft starting, start-up using an inverter drive (VFD), and direct online start-up.

In view of the described difficulties with investigating motors in medium and high-power drive systems, the authors decided to carry out tests on a low-power motor. The study concerned the start-up of a drive system with a 4 kW cage induction motor. To show the differences in the heating of the cast cage winding under different start-up methods, the bar temperature was measured in the slot part. Of course, it must be recognized that high-power cage motors have a different rotor design than smaller motors. It is known that in double cage motors, the highest temperature at start-up is attained by the cage bars outside the core region, while in deep bar motors, the highest bar temperature is found within the core region. In addition, due to the skin effect, there is great variation in the temperature distribution over the cross-section of the bar. The highest temperature occurs in the part of the slot close to the motor's air gap. The temperature of the cage winding during start-up is determined by the quantity of energy released in the winding, irrespective of the size of the motor. According to the simplified analysis of this phenomenon presented in Section 2, the choice of start-up method has a significant effect on the quantity of energy released in the rotor. This finding inspired the authors to investigate this question experimentally.

## 2. Quantity of energy released in the rotor windings of an induction motor during start-up

**2.1. Direct online and soft starting.** To illustrate the phenomenon of energy release in the rotor winding during start-up of an induction motor, the start-up of the drive system is treated as a quasi-stationary state. The energy released in a rotor winding during start-up is expressed by the equation:

$$W_r = \int_0^{t_R} P_r dt = \int_0^{t_R} P_i s dt = \int_0^{t_R} \frac{\omega_s}{p} T s dt, \quad (1)$$

where  $t_R$  is the start-up time,  $s$  is the slip,  $P_r$  is the power released in the rotor winding,  $P_i$  is the power of the rotating field,  $T$  is the torque,  $\omega_s$  is the angular frequency of the stator field, and  $p$  is the number of pole pairs. Combining (1) with the torque equation:

$$T = J \frac{d\Omega_m}{dt} + T_L, \quad (2)$$

where  $T_L$  is the load torque,  $J$  is the moment of inertia, and  $\Omega_m$  is the mechanical angular speed of the rotor, we obtain:

$$W_r = \frac{1}{2} J \left( \frac{\omega_s}{p} \right)^2 (s_1^2 - s_2^2) + \int_0^{t_R} T_L \left( \frac{\omega_s}{p} - \Omega_m \right) dt, \quad (3)$$

where  $s_1$  is the initial slip ( $s_1 = 1$ ), and  $s_2$  is the slip in steady state. If during start-up we have a situation where the load torque can be neglected ( $T_L = 0$ ) and  $s_2 \approx 0$ , the energy released in the rotor winding according to Eq. (3) reduces to:

$$W_r = \frac{1}{2} J \left( \frac{\omega_s}{p} \right)^2. \quad (4)$$

This is equal to the kinetic energy of masses rotating with a synchronous angular speed  $\omega_s/p$ . Equation (4) shows that the energy released in the rotor in the absence of a static load torque, given the stated assumptions, must be the same in case of direct online start-up and soft starting. It depends only on the moment of inertia of the rotating masses and on the final speed. In effect, the temperature field of the motor after the completion of start-up can be expected to be similar for the two start-up methods. When start-up takes place with a large load torque, the second term in Eq. (3) can be depicted as the area above the curve representing the speed of the motor as a function of time (Fig. 1).

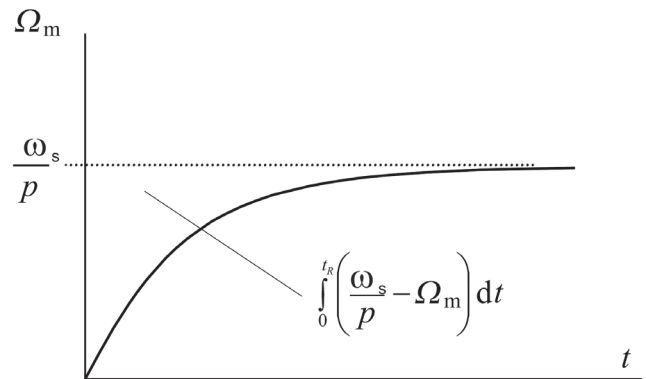


Fig. 1. Illustration of the second term in Eq. (3)

In the case of start-up with a static load torque, the second term in Eq. (3) means that the energy released in the rotor winding in the soft starting case is larger than in the case of direct online start-up, because the start-up time is longer. A higher temperature should then be expected in the rotor. The release of an excessive quantity of energy in the rotor winding during start-up may lead to damage to the cage structure, as a result of thermally induced mechanical stresses exceeding the permissible level.

**2.2. VFD start-up.** In variable-frequency drive (VFD) start-up, assuming the absence of a load torque ( $T_L = 0$ ), and assuming that the selected control method ensures a constant torque

during start-up, the speed during start-up may be taken to vary linearly according to the equation:

$$\Omega_m = \frac{\Omega_{mk}}{t_R} t, \quad (5)$$

where  $\Omega_{mk}$  is the steady-state speed. Hence  $\frac{d\Omega_m}{dt} = \frac{\Omega_{mk}}{t_R}$ .

From (1), (2) and (5) we obtain:

$$W_r = \int_0^{t_R} J \frac{\Omega_{mk}}{t_R} \frac{\omega_s}{p} s dt = \int_0^{t_R} J \frac{\Omega_{mk}}{t_R} \left( \frac{\omega_s}{p} - \Omega_m \right) dt. \quad (6)$$

It can be assumed that during start-up, the linear growth in the rotor speed  $\Omega_m$  will be accompanied by linear growth in the angular frequency of the stator voltage  $\omega_s$  (Fig. 2); and hence the angular speed of the field relative to the rotor  $\frac{\omega_s}{p} - \Omega_m$ , and the slip  $s$ , are approximately constant. Then:

$$\begin{aligned} W_r &= J \Omega_{mk} \left( \frac{\omega_s}{p} - \Omega_m \right) \approx J \frac{\omega_s}{p} (1-s) \frac{\omega_s}{p} s = \\ &= 2W_k (1-s)s, \end{aligned} \quad (7)$$

where  $W_k = \frac{1}{2} J \left( \frac{\omega_s}{p} \right)^2$  is the kinetic energy of the rotor turning with angular speed  $\omega_s/p$ , and  $s$  is the slip resulting from the steady-state speed. Equation (7) implies that the energy released during VFD start-up without a load is significantly lower than the energy released during direct online start-up, given by Eq. (4). The energy released in the rotor will also be lower in the case of start-up subject to a load torque. Assuming that the load torque is constant during start-up, the assumption of a linear increase in speed can be maintained. Then the value of the second term in Eq. (3) is proportional to the area marked in Fig. 2. Compared with the direct online case (Fig. 1), this energy is significantly lower. Hence, in the case of VFD start-up, the thermal stresses on the motor cage can be expected to be significantly smaller than with direct online start-up.

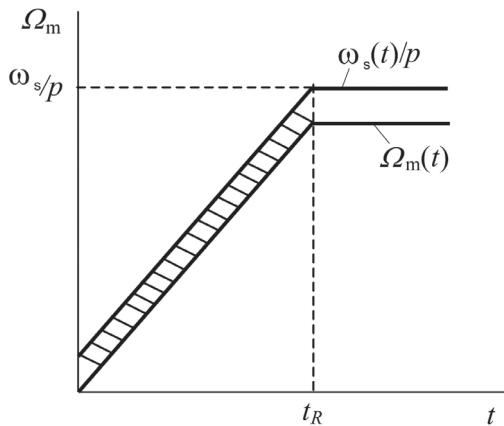


Fig. 2. Change of rotor angular speed  $\Omega_m$  and the angular speed of the rotating field  $\omega_s/p$  during VFD start-up

### 3. Description of experiments

**3.1. Measuring stand.** A block diagram of the laboratory stand is shown in Fig. 3. Experiments were performed on an SEE112M-4 induction motor with the characteristics given in Table 1.

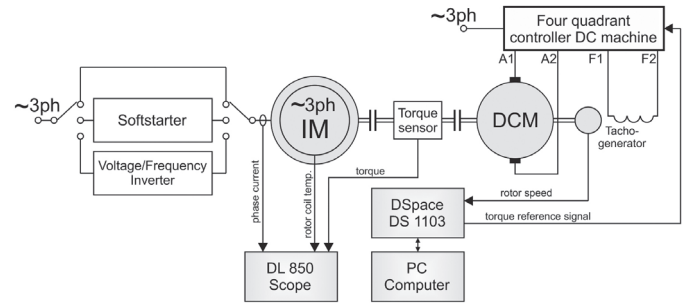


Fig. 3. Block diagram of the experimental stand

Table 1  
Chosen parameters of tested motor

Parameter	Value
Rated power, kW	4
Rated voltage, V	400 Δ
Rated frequency, Hz	50
Rated current, A	8.1
Efficiency, %	88.3
Power factor	0.81
Class of insulation	F

The motor was loaded with a PROZc 160 SX separately excited DC generator with power 5.5 kW, which was connected to a Mentor MP controller. The controller operated in torque control mode. The load torque characteristic was dependent on the rotational speed of the rotor and is plotted in Fig. 4. The torque was controlled using a DS1103 card, in which the load torque characteristic had been programmed (Fig. 4). The load torque control signal was then converted to an analogue signal and fed to the input of the Mentor MP controller. An additional moment of inertia was attached to the generator shaft.

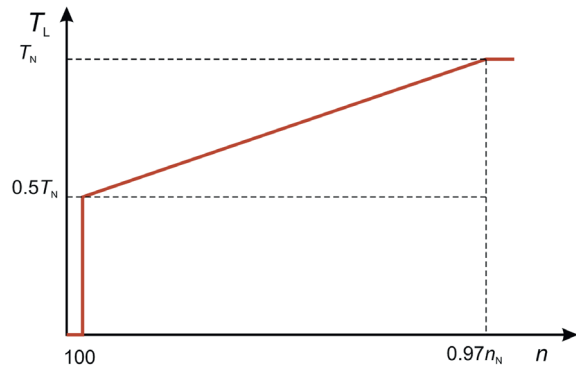


Fig. 4. Motor load torque characteristic

The torque was measured using a Megatron DFM2x torque sensor, shown in Fig. 5. The temperature of a bar of the rotor cage was measured using a CuKo thermocouple pressed into the material of the bar in the core region of the cage, in the part of the slot next to the air gap (Fig. 6). The signal from the thermocouple was transmitted via a Vibro-Meter 4-MTA/T rotary joint. A view of the testing stand is presented in Fig. 7.

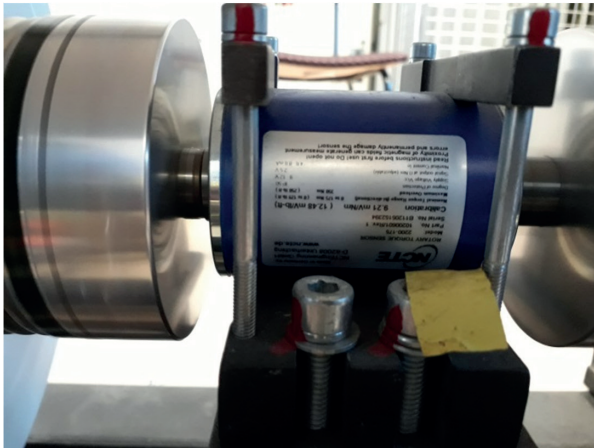


Fig. 5. Torque sensor



Fig. 6. Place of mounting of the thermocouple used to measure the temperature of a bar of the cage winding

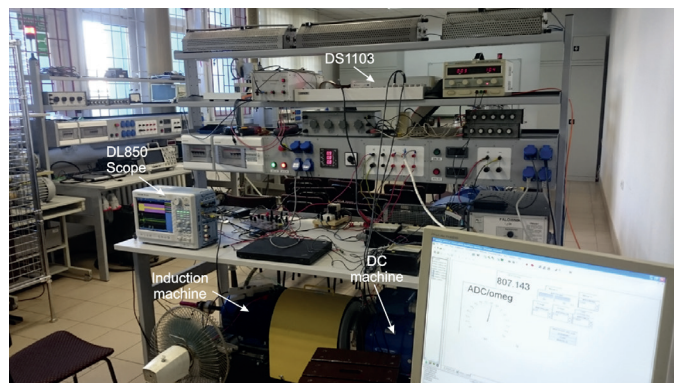


Fig. 7. Experimental stand

The signals representing the bar temperature and motor current and the signal from the torque sensor were recorded using a Yokogawa DL 850 ScopeCorder. Direct online start-up was carried out by connecting the motor directly to the power supply network, with measurement of the stator current, the torque, the speed, and the cage winding bar temperature. Soft starting was carried out by powering the motor from a Danfoss MCD500 soft starter. In the case of VFD start-up the motor was powered by a Control Techniques Unidrive SP 2401 inverter. The load torque characteristic was identical for all tested start-up methods.

**3.2. Measurement results.** Using the measurement stand described in Section 3.1, measurements of torque, rotor speed, stator current and cage bar temperature were recorded for all of the following cases:

- direct online start-up (with the motor connected to the full network voltage),
- soft starting,
- start-up using an inverter (VFD start-up).

The mechanical load characteristic was identical in all cases. The initial load torque was selected to enable soft starting of the motor, and the torque then increased in proportion to the rotor speed up to the rated value in steady operating state. The moment of inertia of the system also remained invariable. The plots show relative values of the recorded quantities. In the case of torque and speed, the baselines are the steady-state values. For stator current, the baseline is its amplitude in steady state. The baseline temperature was taken to be the initial temperature of the rotor cage bar, which was equal to room temperature in all cases.

Figure 8 shows plots of the measured values of torque, speed, stator current and rotor cage bar temperature when the motor was connected to the full network voltage (direct online start-up).

Figure 9 shows plots of the measured values of torque, speed, stator current and rotor cage bar temperature when the motor underwent soft starting. The soft starter operated with a current limit of 450% of the rated current.

Compared with the direct online case, it is notable that there is a significant decrease in the initial starting torque, to a value of approximately  $0.6T_N$  (for direct online start-up the value was around  $2T_N$ ). The cage winding bar temperature at the end of start-up is significantly higher than in the direct online case, with a relative value (per unit quantities) of approximately 1.3 (compared with 1.05 for direct online start-up). The difference between speed response in the case of soft starting (Fig. 9) and direct start-up (Fig. 8) is also noticeable.

A positive consequence of the use of a soft starter is clearly the reduction of the starting current to a value of approximately  $4I_N$  (compared with around  $6I_N$  in the direct online case).

Figure 10 shows plots of the measured values of torque, speed, stator current and rotor cage bar temperature when the motor was started using an inverter (VFD start-up). The VFD operated with an acceleration gradient of  $8 \text{ s}/100 \text{ Hz}$ . The results illustrated in Fig. 10 show that the use of VFD start-up did not cause a significant rise in the temperature

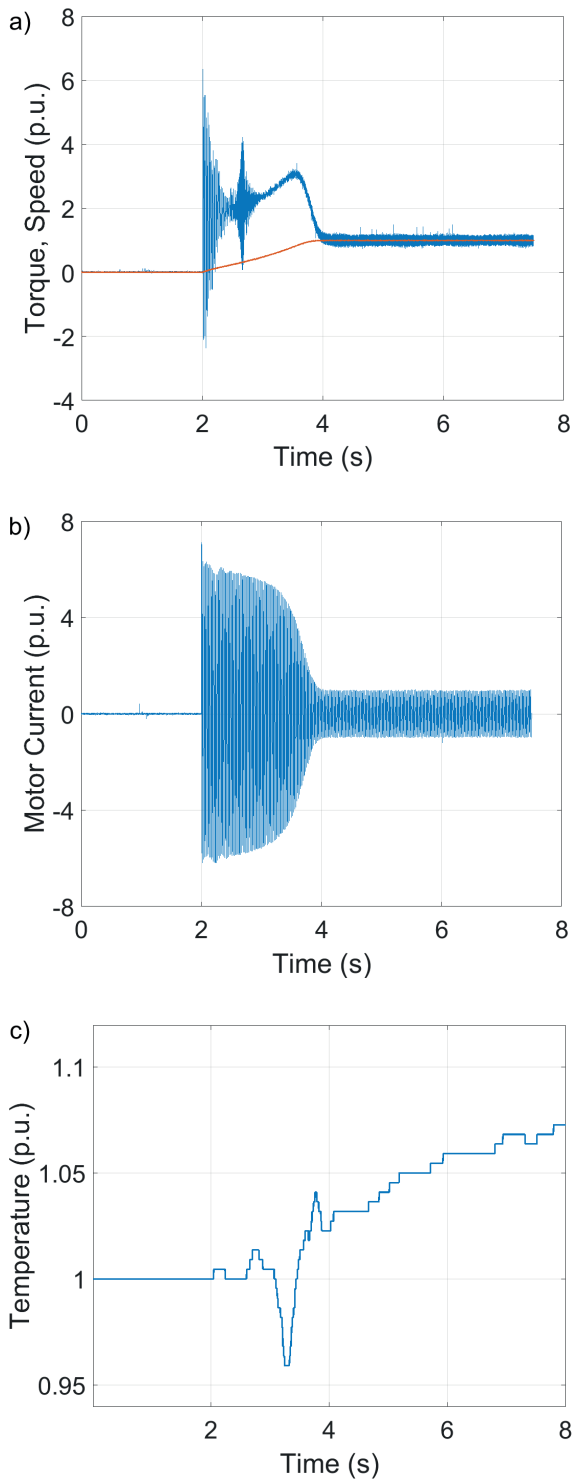


Fig. 8. Plots of measured values of (a) torque and speed, (b) stator current, and (c) rotor cage bar temperature during direct online start-up

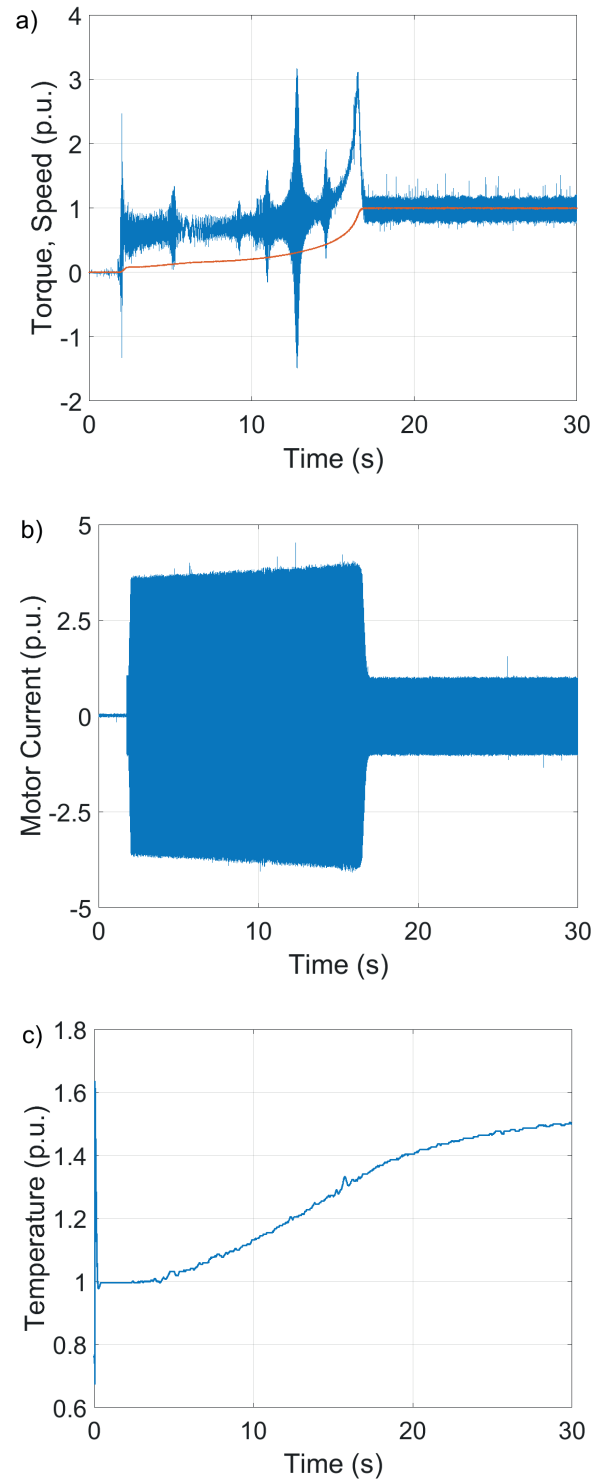


Fig. 9. Plots of measured values of (a) torque and speed, (b) stator current, and (c) rotor cage bar temperature during soft starting

of the bar of the cage winding. Moreover, the starting current was significantly reduced (to a value of approximately  $1.6I_N$ ). Figure 11 shows a comparison of the cage winding bar temperature during start-up by different methods and for a short time of steady-state operation after start-up. It is seen that the final temperature is highest in the case of soft

starting, when it is approximately 34% higher than in the case of direct online start-up. This implies a lowering of the resistance of the cage winding to repeated start-up. In the case of VFD start-up the observed temperature value was the smallest, being around 7% lower than in the direct online case.

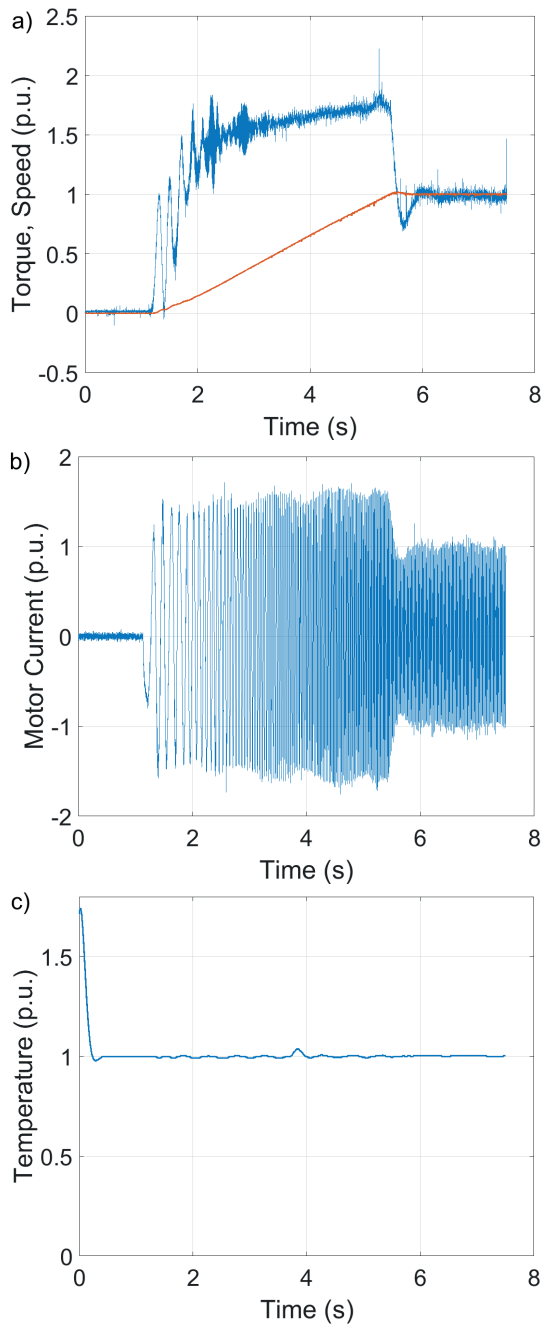


Fig. 10. Plots of measured values of (a) torque and speed, (b) stator current, and (c) rotor cage bar temperature during start-up using a VFD with a ramp of 8 s/100 Hz

### 1. Risk of damage to high-power motors

The described laboratory experiments only partially confirm the hypotheses put forward in Section 2 concerning the energy released in the rotor windings of an induction motor during start-up. For technical reasons, it was not possible to obtain start-up times sufficiently long that the temperature of elements of the cage winding would pose a risk to its durability. In high-power motors, prolonged start-up causes elements of the cage winding to attain temperatures of several hundred degrees.

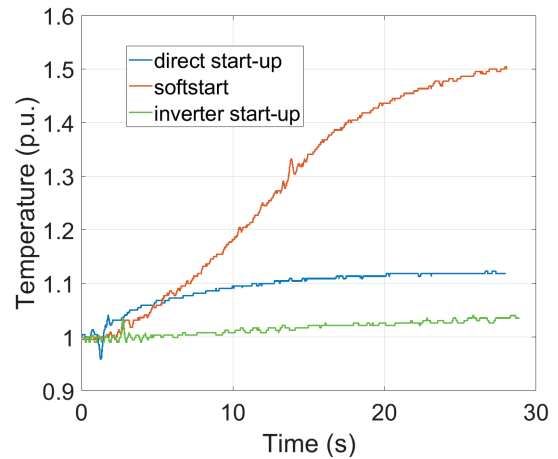


Fig. 11. Change of cage winding bar temperature during start-up by different methods and for a short time of steady-state operation after start-up

Figure 12 shows a simulated spatiotemporal temperature distribution along the axis of a bar of the starting cage during direct online start-up of a 320 kW double cage motor, in the case  $T_L \neq 0$  [22]. This process leads to high thermal stresses in the cage structure, increasing the probability of damage to the rotor windings.

### 2. Conclusions

The laboratory tests showed that the use of a soft starter reduces the motor's starting current but prolongs the start-up time and increases the rotor winding temperature. The advantage, there-

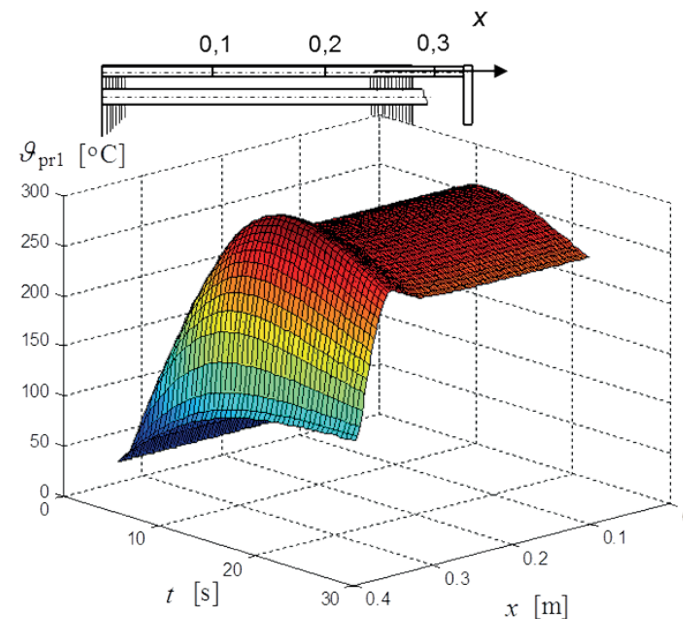


Fig. 12. Spatiotemporal distribution of temperature along the axis of a starting cage bar during direct online start-up of a 320 kW double cage motor in the case  $T_L \neq 0$

fore, is a reduction in the danger to the motor resulting from the electrodynamic effect of the starting current and its action on the power supply network. Nevertheless, the use of a soft starter also carries some negative consequences. The significant decrease in the initial starting torque causes an increase in start-up time. In the case of soft starting with a static load torque the cage bar temperature is significantly higher, because much more energy is released in the rotor cage winding than during direct online start-up. Therefore, using a soft starter does not reduce the thermal effects occurring in the motor during start-up when subject to load torque. VFD start-up substantially reduces the thermal risk to the durability of the cage, as the quantities of energy released in the rotor winding are significantly smaller, and consequently the measured cage bar temperature is lower, than in the case of other start-up methods.

The research described concerns a low-power cage motor. It may be expected that in the start-up of medium- and high-power cage motors, the phenomena observed here will occur with greater intensity, in relation to the use of deep bar and double cage rotors.

These types of rotors make use of the skin effect, and hence the cage winding of a high-power motor heats up in a highly non-uniform manner. The results obtained here indicate that there is a particular need for research into the energy aspects of different start-up methods for medium and high-power cage motors. Given the relatively small number of publications reporting on expensive experimental testing of high-power motors, there is a need to plan and carry out such testing in order to provide verification of simulation models and to enable further improvements in the design of cage windings.

**Acknowledgements.** This work is financed by the statutory funds (UPB) of the Department of Electrodynamics and Electrical Machine Systems, Rzeszow University of Technology.

## REFERENCES

- [1] Y. Gritli, S.B. Lee, F. Filippetti, and L. Zarri, “Advanced diagnosis of outer cage damage in double-squirrel-cage induction motors under time-varying conditions based on wavelet analysis”, *IEEE Trans. Ind. Appl.* 50(3), 1791–1800, (2014).
- [2] Y. Gritli, O. Di. Tommaso, R. Miceli, F. Filippetti, and C. Rossi, “Vibration signature analysis for rotor broken bar diagnosis in double cage induction motor drives”, *4th International Conference on Power Engineering, Energy and Electrical Drives*, Istanbul, Turkey, 2013, pp. 1814–1820.
- [3] F. Wilczyński, P. Strankowski, J. Guziński, M. Morawiec, and A. Lewicki, “Sensorless field oriented control for five-phase induction motors with third harmonic injection and fault insensitive feature”, *Bull. Pol. Acad. Sci. Tech. Sci.* 67(2), 253–262, (2019).
- [4] C.G. Dias, L.C. da Silva, and I. E. Chabu, “Fuzzy-based statistical feature extraction for detecting broken rotor bars in line-fed and inverter-fed induction motors”, *Energies* 12(12), 2381, (2019).
- [5] T. Nakahama, D. Biswas, K. Kawano, and F. Ishibashi, “Improved cooling performance of large motors using fans”, *IEEE Transactions on Energy Conversion*, 21(2), 324–331, (2006).
- [6] D. Staton, A. Boglietti, and A. Cavagnino, “Solving the more difficult aspects of electric motor thermal analysis in small and medium size industrial induction motors”, *IEEE Trans. Energy Convers.* 20(3), 620–628, (2005).
- [7] C. Ulu, O. Korman, and G. Komurgoz, “Electromagnetic and thermal design/analysis of an induction motor for electric vehicles”, *2017 8th International Conference on Mechanical and Aerospace Engineering (ICMAE)*, Prague, Czech Republic, 2017.
- [8] Y. Xie, J. Guo, P. Chen, and Z. Li, “Coupled fluid-thermal analysis for induction motors with broken bars operating under the rated load”, *Energies*, 11(8), 2024, (2018).
- [9] K.N. Gyftakis, D. Athanasopoulos, and J. Kappatou, “Study of double cage induction motors with different rotor bar materials”, *20th International Conference on Electrical Machines (ICEM)*, Marseille, France, 2012, pp. 1450–1456.
- [10] Z. Maddi and D. Aouzellag, “Dynamic modelling of induction motor squirrel cage for different shapes of rotor deep bars with estimation of the skin effect”, *Prog. Electromagn. Res. M* 59, 147–160, (2017)
- [11] M. Sundaram, M. Mohanraj, P. Varunraj, T.D. Kumar, and S. Sharma, “FEA based electromagnetic analysis of induction motor rotor bars with improved starting torque for traction applications”, *Proceedings of the International Conference on Automatic Control, Mechatronics and Industrial Engineering (ACMIE)*, Suzhou, China, 2018.
- [12] H.J. Lee, S.H. Im, D.Y. Um, G.S. Park, “A design of rotor bar for improving starting torque by analyzing rotor resistance and reactance in squirrel cage induction motor”, *IEEE Trans. Magn.* 99, 1–4, (2017).
- [13] L. Livadaru, A. Simion, A. Munteanu, M. Cojan, and O. Dabija, “Dual cage high power induction motor with direct start-up design and FEM analysis” *Adv. Electr. Comput. Eng.* 13(2), 55–58, (2013).
- [14] S. Sinha, N.K. Deb, and S.K. Biswas, “The design and its verification of the double rotor double cage induction motor”, *Journal of The Institution of Engineers (India): Series B* 98(1), 107–113, (2017).
- [15] W. Poprawski and T. Wolnik, “Innovative design of double squirrel cage induction motor for high start frequency operation”, *Electr. Mach. Trans. J. Inst. Electr. Drives Mach. KOMEL* 111(3), 41–44, (2016).
- [16] J. Mróz and W. Poprawski, “Improvement of the Thermal and Mechanical Strength of the Starting Cage of Double-Cage Induction Motors”, *Energies* 12 (23), 4551, (2019).
- [17] J. Mróz, “Start-up of the Deep-Bar Motor with the use of the Softstart-up – An Energetisitec Face”, *Zeszyty Problemowe BOBRME Komel* 81, 17–22, (2009) [in Polish].
- [18] J. Mróz, “Energy Emitted in the Induction Motor’s Winding During the Start-up with the use of the Softstart-up”, *Zeszyty Problemowe BOBRME Komel*, 84, 121–126, (2009) [in Polish].
- [19] M.G. Solveson, B. Mirafazal, and N.A.O. Demerdash, “Soft-Started Induction Motor Modeling and Heating Issues for Different Starting Profiles Using a Flux Linkage ABC Frame of Reference”, *IEEE Trans. Ind. Appl.* 42(4), 973–982, (2006)
- [20] R. Krok, “Influence of work environment on thermal state of electric mine motors”, *Arch. Electr. Eng.* 60(3), 357–370, (2011).
- [21] Q. Al’Akayshee and D.A. Staton, “1150 hp motor design, electromagnetic and thermal analysis”, *ICEM – 15-th International conference on electrical machines*, Bruges, Belgium, 2002.
- [22] J. Mróz, *The Analysis of Coupled Electromechanical and Thermal Problems in Transient States of Double-Cage Induction Motors*, Publishing House Rzeszow University of Technology: Rzeszow, Poland, 2013, [in Polish].